PERGAMON

International Journal of Heat and Mass Transfer 43 (2000) 1457–1467

International Journal of HEAT and MASS TRANSFER

www.elsevier.com/locate/ijhmt

Analytical solutions to the unsteady close-contact melting on a flat plate

Hoseon Yoo

Department of Mechanical Engineering, Soong Sil University, Seoul 156-743, South Korea

Received 29 October 1998; received in revised form 12 May 1999

Abstract

This work reports a set of approximate analytical solutions describing the transient process of gravity-induced close-contact melting between a rectangular parallelepiped solid and a flat plate on which either constant temperature or constant heat flux is imposed. Not only relative motion of the solid block tangential to the heating plate, but also the solid–liquid density difference is incorporated in the model. Normalization of the model equations in reference to the steady state admits compactly expressed analytical solutions, which agree excellently with the available numerical data. Based on the normalized liquid film thickness that is independent of the parameters, the transient time duration of close-contact melting is defined uniquely. The present solution is also capable of resolving distinctive behaviors of the solid descending velocity at the early stage of melting. A geometric function characterizing the three-dimensional effect is introduced, and its properties are clarified. It is found in the case of constant contact area that as the cross-sectional shape deviates from square, heat transfer is at least enhanced at the expense of the increase in friction between two solids. © 2000 Elsevier Science Ltd. All rights reserved.

Keywords: Close-contact melting; Analytical solution; Aspect ratio; Melt lubrication

1. Introduction

Close-contact melting is a basic phase change phenomenon occurring at the interface of two solid bodies in contact, one of which is heated above the melting temperature of the other. It is involved in various natural and technological processes [1]. From the engineering viewpoint of primary interest are high heat transfer rate due to direct contact and/or low friction by the action of the liquid film formed between the two solids. These features have already been or are to be applied to some practical systems such as latent heat storage, melt lubrication and burial of heat generating bodies [2].

During the past several decades, numerous researches on contact melting processes have been conducted for diverse geometrical configurations, heat supplying modes, contact conditions and types of relative motion between two solids, which have recently been reviewed by Bejan [3]. According to this review, theoretical models adopted for analyzing close-contact melting phenomena have exclusively relied on the assumption of quasi-steady state. That is, most of the previous works have performed the steady analysis. In view of an experimental result [1], the initial transient process from the onset to the quasi-steady state seems to be short compared

E-mail address: hsyoo@engineer.soongsil.ac.kr (H. Yoo).

0017-9310/00/$ - see front matter © 2000 Elsevier Science Ltd. All rights reserved.
PII: S0017-9310(99)00221-5

Nomenclature

A	aspect ratio of contact surface, W/L
c	liquid specific heat
f	friction coefficient, $F_x/(Mg)$
F	force
g	gravitational acceleration
$\tilde{g}$	dimensionless acceleration, gR^3/α^2
G	geometric function, G'/A
G'	geometric function, Eq. (17)
h_{sf}	latent heat of fusion
H	height of the solid block
$\tilde{H}$	dimensionless height, H/R
k	liquid thermal conductivity
K_n	coefficients, Eq. (A8)
L	sliding-contact length, Fig. 1
M	mass of the solid block
n	non-negative integer
P	pressure in the liquid film
P_1, P_2	decomposed variables, Eqs. (A3)–(A5)
Pr	Prandtl number, $\mu c/k$
q_w	wall heat flux
$\tilde{q}_w$	dimensionless heat flux, $q_w R/(\alpha\rho_s h_{sf})$
Q	volume flow rate
r	radius of circular cross-section
R	characteristic length
S	source term
Ste	Stefan number, $c(T_w - T_m)/h_{sf}$
t	time
$\tilde{t}$	dimensionless time, $t\alpha/R^2$
$\hat{t}$	normalized time, $\tilde{t}\tilde{V}_c/(\tilde{\rho}\tilde{\delta}_c)$
T	temperature
T_m, T_w	melting and wall temperature
u, v, w	velocity components, Fig. 1
U	velocity of relative motion
$\tilde{U}$	dimensionless relative velocity, UR/α
V	solid descending velocity
$\tilde{V}$	dimensionless descending velocity, VR/α
$\hat{V}$	normalized descending velocity, $\tilde{V}/\tilde{V}_c$
W	depth of the solid block, Fig. 1
x, y, z	Cartesian coordinates, Fig. 1

Greek symbols

α	liquid thermal diffusivity, $k/(\rho_l c)$
β_n	eigenvalues, Eq. (A7)
δ	liquid film thickness
$\tilde{\delta}$	dimensionless thickness, δ/R
$\hat{\delta}$	normalized thickness, $\tilde{\delta}/\tilde{\delta}_c$
μ	viscosity
ρ	density
$\tilde{\rho}$	density ratio, ρ_l/ρ_s

Subscripts

c	steady state
l	liquid phase
s	solid phase
u	unsteady period
x, y	x, y direction

with the whole close-contact melting. However, in order to estimate whether the transient process can be neglected or not, and to predict the transient response of system to the change in imposed conditions during a certain steady melting, the unsteady analysis is needed. In addition, thorough understanding of the transient behavior itself would deserve research attention in close-contact melting area.

Few unsteady analysis has recently been reported in the open literature. Hong and Saito [4] appears to be the first to investigate the initial transient process as a separate subject. Using a sophisticated model, they numerically solved full governing equations for unsteady two-dimensional flow and heat transfer during close-contact melting between ice kept at its freezing temperature and an isothermally heated flat plate. The same method has also been applied to the case of constant wall heat flux [5]. These studies are worth addressing in that they initiatively developed a numerical method for predicting the unsteady behavior, but seems to be insufficient for resolving the basic characteristics such as the transient time duration. If an analytical solution to the unsteady close-contact melting were available, it would not only serve as a reference to validate numerical simulations, but also be convenient for estimating the limitation involved in steady analyses.

Based on the well-known analytical approaches to quasi-steady problems [1,2,6,7], the present study is intended to derive a set of analytical solutions for a simplified model of the unsteady close-contact melting. For ease of the analysis, presumed are that the phase change material is kept at its melting temperature, and that the heating plate is flat and horizontal, as have been commonly done in the previous studies [2,4,5]. The geometry of the solid block considered here is a rectangular parallelepiped, so that the phenomenon takes place three-dimensionally [2]. The analysis covers both the cases of constant wall temperature and constant wall heat flux heating in the same framework. Moreover, the model accounts for not only the density difference between the solid and liquid phases, but also relative motion of the solid block tangential to the heating plate. In order to assess the simplifications

introduced in modeling, the obtained results are compared with the afore-mentioned numerical simulations [4,5]. The discussion encompasses key features of the analytical solutions, and the effect of the aspect ratio of sliding-contact surface is highlighted.

2. Modeling

The physical system considered in this work is depicted schematically in Fig. 1 together with the coordinates. A rectangular parallelepiped solid block of size $L \times W \times H$ at its melting temperature T_m begins to melt from $t = 0$ on the heating plate that moves at a constant relative velocity U in the x direction due to the tangential force F_x, while being in contact with the plate by its own weight. There is no fundamental difference in the analysis when contact is maintained by the externally applied vertical force as in other works [2,8] instead of the gravity. As the melting proceeds, a part of the liquid generated along the phase change front fills up the growing gap between the block and plate, and the rest is enforced to flow and to be squeezed out through the peripheral openings around the contact area by the solid descending motion. Both of the liquid film thickness δ and the solid descending velocity V vary with time, and eventually attain the quasi-steady state where the melting rate coincides with the solid descending velocity. Since the friction exerted on the contact area also varies during this process, the tangential force F_x should be adjusted such that the velocity U is kept constant.

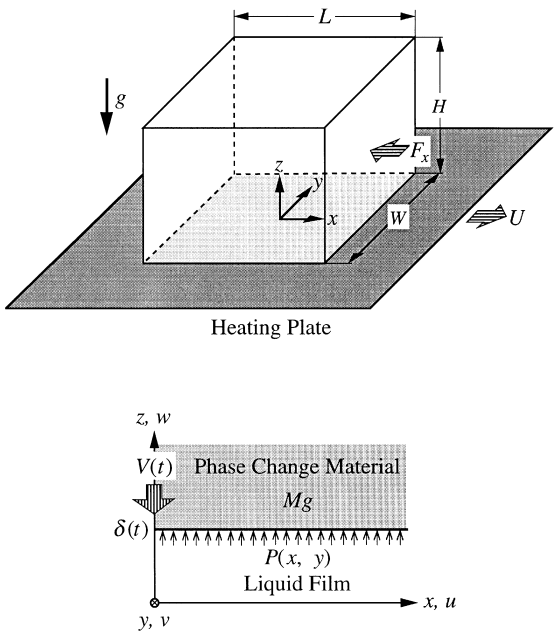

Fig. 1. Schematic of the present close-contact melting system.

The present study is aimed at analyzing those transient behaviors from the onset to the steady state of close-contact melting. Transition from one steady contact melting to another caused by a certain change in the imposed conditions belongs to the same category of problems. As described before, the analysis is performed for two representative heating modes: constant wall temperature and constant wall heat flux.

Despite relatively simple geometry, the phenomenon is three-dimensional. In order to approach the problem analytically, some simplifications have been introduced within the extent of preserving the fundamental features of close-contact melting. First, neglected are both the heat generated by friction between direct contact solids before the beginning of melting and viscous dissipation of the flow in the liquid film after melting. This is valid if the relative velocity between the solid block and plate is not high [9]. A situation where frictional heat or viscous dissipation is dominant should be treated as a separate topic [2]. Second, the tangential force F_x acts in a way that the solid block does not rotate about both the y and z axes [9]. Third, the thin film approximation holds for the liquid layer throughout the whole process. The approximation states that the transverse diffusion predominates over the longitudinal diffusion as well as the inertia and convection, and the pressure in the film is uniform in the crosswise direction [10]. Even in the steady close-contact melting, the effect of convection relative to conduction turned out to be negligible for $Ste < 0.1$ [11,12]. The second and third assumptions yield a uniform liquid film thickness over the contact area [2]. Finally, the mass of solid block is assumed to be invariant during the transient process. It seems to be reasonable that the effect of mass variation is not significant in the practical conduction-dominated process unless the initial height of the block is very small compared with the length scale of contact area. Moallemi et al. [1] showed that the criteria of $H/r > 0.1$ (where r is the radius of circular cross-section) and $Ste < 0.1$ ensure the validity of this assumption.

Regardless of the heating mode and the existence of relative motion, the transient behavior of close-contact melting is characterized by the timewise variations of solid descending velocity and liquid film thickness, i.e. $V(t)$ and $\delta(t)$, respectively. These dependent variables are to be determined such that they satisfy the following force and energy balances simultaneously. First, the weight and inertia of the solid block, and the pressure in the liquid film are related as [1,4]

$$M\left(g - \frac{dV}{dt}\right) = \int_{-W/2}^{W/2}\int_{-L/2}^{L/2} P(x, y)\, dx\, dy \tag{1}$$

Since the acceleration of the solid block, dV/dt, is much smaller than that of the gravity, g, in conventional systems, it is neglected here additionally [1]. Next, the energy balance at the solid–liquid interface is expressed as

$$-k\left.\frac{\partial T}{\partial z}\right|_{z=\delta} = \rho_s h_{sf}\left(V + \frac{d\delta}{dt}\right) \tag{2}$$

The term in bracket of Eq. (2) represents the unsteady melting rate which is composed of the solid descending velocity and the growth rate of film thickness. One thing to remark here is that the contribution of these two terms to the pressure rise differ from each other (this is clarified later).

Meanwhile, the tangential force responsible for relative motion can be obtained from the total shear force of the liquid film as [2]

$$F_x = -\int_{-W/2}^{W/2}\int_{-L/2}^{L/2} \mu\left.\frac{\partial u}{\partial z}\right|_{z=0} dx\, dy \tag{3}$$

3. Analysis

3.1. Model equations

For the closure of Eqs. (1)–(3), we have to express the pressure in the liquid film, interfacial temperature gradient, and velocity gradient along the plate in terms of the dependent variables. This can be done by solving the continuity, momentum, and energy equations in the liquid film. Owing to the thin film approximation, they are simplified as [2]

$$\frac{\partial u}{\partial x} + \frac{\partial v}{\partial y} + \frac{\partial w}{\partial z} = 0 \tag{4}$$

$$\frac{\partial P}{\partial x} = \mu\frac{\partial^2 u}{\partial z^2} \tag{5}$$

$$\frac{\partial P}{\partial y} = \mu\frac{\partial^2 v}{\partial z^2} \tag{6}$$

$$\frac{\partial^2 T}{\partial z^2} = 0 \tag{7}$$

Since the temperature is still a function of t as well as z due to the moving interface, i.e. $\delta(t)$, Eq. (7) retains the partial derivative. The boundary conditions for velocity components are

$$u = U; \qquad v = w = 0 \quad \text{at } z = 0 \tag{8}$$

$$u = v = 0; \qquad w = -\frac{\rho_s}{\rho_l}V - \frac{\rho_s - \rho_l}{\rho_l}\frac{d\delta}{dt} \text{ at } z = \delta \tag{9}$$

It should be remarked that the condition for w in Eq. (9) reflects the effect of solid–liquid density difference. The first and second terms on its right-hand side denote the blowing of liquid due to the descending solid and the excess or deficient volume due to the film growth, respectively. As for the temperature, the boundary conditions are evidently $T = T_w$ (constant wall temperature) or $-k(\partial T/\partial z) = q_w$ (constant heat flux) at $z = 0$, and $T = T_m$ at $z = \delta$.

Since the pressure distribution in the liquid film, $P(x, y)$, has already been derived [2], the procedure is condensed here. Solving Eqs. (5) and (6) subject to the boundary conditions (8) and (9), we get

$$u(x, y, z) = \frac{1}{2\mu}\left(\frac{\partial P}{\partial x}\right)z(z - \delta) + U\left(1 - \frac{z}{\delta}\right) \tag{10}$$

$$v(x, y, z) = \frac{1}{2\mu}\left(\frac{\partial P}{\partial y}\right)z(z - \delta) \tag{11}$$

These allow us to obtain the x and y directional volume flow rates through the film,

$$Q_x = \int_0^\delta u\, dz = \frac{1}{12\mu}\left(-\frac{\partial P}{\partial x}\right)\delta^3 + \frac{1}{2}U\delta \tag{12}$$

$$Q_y = \int_0^\delta v\, dz = \frac{1}{12\mu}\left(-\frac{\partial P}{\partial y}\right)\delta^3 \tag{13}$$

respectively. Substitution of Eqs. (12) and (13) into the continuity equation integrated with respect to z, i.e.

$$\frac{\partial Q_x}{\partial x} - \left(\frac{\rho_s}{\rho_l}V + \frac{\rho_s - \rho_l}{\rho_l}\frac{d\delta}{dt}\right) + \frac{\partial Q_y}{\partial y} = 0 \tag{14}$$

results in the following partial differential equation for $P(x, y)$:

$$\frac{\partial^2 P}{\partial x^2} + \frac{\partial^2 P}{\partial y^2} = -\frac{12\mu}{\delta^3}\left(\frac{\rho_s}{\rho_l}V + \frac{\rho_s - \rho_l}{\rho_l}\frac{d\delta}{dt}\right) \tag{15}$$

Note that the right-hand side of Eq. (15) is independent of x and y.

Assuming that the pressure in the film equilibrates with that of the environment along the periphery of contact surface irrespectively of relative motion [2], the boundary conditions for Eq. (15) are homogeneous, i.e. $P(\pm L/2, \pm W/2) = 0$. It is a known fact that the Poisson equation subject to such conditions admits an exact solution [2]. The derivation procedure is summarized in Appendix A. By substituting Eq. (A6) into Eq. (1), the force balance reduces to

$$\rho_s LWHg = \frac{\mu L^3 W}{\delta^3}\left(\frac{\rho_s}{\rho_l}V + \frac{\rho_s - \rho_l}{\rho l}\frac{d\delta}{dt}\right)G' \tag{16}$$

where G' is a function of the aspect ratio of contact area, A, and defined as

$$G'(A) = 1 - \frac{192}{\pi^5 A}\sum_{n=0}^{\infty}\frac{\tanh\left[(2n+1)\pi A/2\right]}{(2n+1)^5} \tag{17}$$

The function proved to have the property of $G'(\infty)\to 1$ and $G'(0)\to A^2$ [2].

The interfacial temperature gradient can be readily determined from Eq. (7), so that the energy balance for each of the heating modes is rewritten as

$$\frac{k(T_w - T_m)}{\delta} = \rho_s h_{sf}\left(V + \frac{d\delta}{dt}\right) \tag{18}$$

$$q_w = \rho_s h_{sf}\left(V + \frac{d\delta}{dt}\right) \tag{19}$$

respectively. For the later use, the dependence of the wall temperature variation for constant heat flux on the film thickness is identified here as

$$T_w(t) = T_m + \frac{q_w \delta(t)}{k} \tag{20}$$

Using the known velocity profile, Eq. (10), we can simplify Eq. (3) as

$$F_x = \frac{\mu U L W}{\delta} \tag{21}$$

The tangential force driving relative motion is expressed in terms of the liquid film thickness. In consequence, the system of model equations for determining the dependent variables $V(t)$ and $\delta(t)$ consists of two simultaneous first-order ordinary differential equations Eqs. (16) and (18) or (19). Note that the model equations reduce to algebraic ones in the steady analysis.

3.2. Nondimensionalization and normalization

In order to verify the characteristic parameters pertinent to the present system, the model equations are nondimensionalized. Let the characteristic length be R, then Eq. (16) can be rewritten in terms of the dimensionless quantities defined in Nomenclature as

$$\left[\tilde{V} + (1-\tilde{\rho})\frac{d\tilde{\delta}}{d\tilde{t}}\right]\left(\frac{L}{R}\right)^2 G' = \left(\frac{\tilde{g}\tilde{H}}{Pr}\right)\tilde{\delta}^3 \tag{22}$$

Depending on the type of applications, a convenient length scale can be taken. Here, we tentatively adopt $R = (LW)^{1/2}$ as the characteristic length, since it seems to be appropriate for examining the effect of aspect ratio under constant contact area. This leads Eq. (22) to

$$\tilde{V} + (1-\tilde{\rho})\frac{d\tilde{\delta}}{d\tilde{t}} = \left(\frac{\tilde{g}\tilde{H}}{GPr}\right)\tilde{\delta}^3 \tag{23}$$

where $G = G'/A$. The dimensionless forms of Eqs. (18) and (19) become independently of the length scale,

$$\tilde{V} + \frac{d\tilde{\delta}}{d\tilde{t}} = \frac{\tilde{\rho} Ste}{\tilde{\delta}} \tag{24}$$

$$\tilde{V} + \frac{d\tilde{\delta}}{d\tilde{t}} = \tilde{\rho}\tilde{q}_w \tag{25}$$

respectively. Note that the three-dimensionality is relevant only to the force balance through a geometric function $G(A)$.

For ease and generalization of the analysis by eliminating the parameters appeared in Eqs. (23) and (24) or (25) as far as possible, attempted is normalization in reference to the steady solution. Since $d\tilde{\delta}/d\tilde{t} = 0$ in the steady state, each set of solutions for the two heating modes is readily derived, respectively, as follows:

$$\tilde{V}_c = \left(\frac{\tilde{g}\tilde{H}}{G\,Pr}\right)^{1/4}(\tilde{\rho}\,Ste)^{3/4}, \qquad \tilde{\delta}_c = \left(\frac{\tilde{g}\tilde{H}}{G\,Pr}\right)^{-1/4}(\tilde{\rho}\,Ste)^{1/4} \tag{26}$$

$$\tilde{V}_c = \tilde{\rho}\tilde{q}_w, \qquad \tilde{\delta}_c = \left(\frac{\tilde{g}\tilde{H}}{G\,Pr}\right)^{-1/3}(\tilde{\rho}\tilde{q}_w)^{1/3} \tag{27}$$

where the subscript c denotes the steady-state. According to the definition of normalized variables, Eqs. (23)–(25) further reduce to

$$\hat{V} + \frac{(1-\tilde{\rho})}{\tilde{\rho}}\frac{d\hat{\delta}}{d\hat{t}} = \hat{\delta}^3 \tag{28}$$

$$\hat{V} + \frac{1}{\tilde{\rho}}\frac{d\hat{\delta}}{d\hat{t}} = \hat{\delta}^{-1} \tag{29}$$

$$\hat{V} + \frac{1}{\tilde{\rho}}\frac{d\hat{\delta}}{d\hat{t}} = 1 \tag{30}$$

respectively. Note that the normalized model equations include the density ratio only, and are far more compact in expression than the dimensionless counterparts.

3.3. Analytical solutions

Each set of normalized equations for the two heating modes can be readily solved to yield an analytical solution. For the case of constant wall temperature, we can derive a differential equation for $\hat{\delta}$ by eliminating $\hat{V}$ from Eqs. (28) and (29),

$$\frac{\mathrm{d}\hat{\delta}^2}{\mathrm{d}\hat{t}} = 2\left(1-\hat{\delta}^4\right) \tag{31}$$

Solving Eq. (31) along with the initial condition, $\hat{\delta}(0)=0$, results in

$$\hat{\delta}(\hat{t}) = \tanh^{1/2}(2\hat{t}) \tag{32}$$

It is easy to express $\hat{V}(\hat{t})$ in terms of $\hat{\delta}(\hat{t})$ from Eqs. (28) and (29) as

$$\hat{V}(\hat{t}) = \frac{\tilde{\rho}-1}{\tilde{\rho}\hat{\delta}} + \frac{\hat{\delta}^3}{\tilde{\rho}} \tag{33}$$

Note that Eq. (33) reduces to an explicit function of $\hat{t}$ when $\tilde{\rho}=1$, i.e.

$$\hat{V}(\hat{t}) = \tanh^{3/2}(2\hat{t}) \tag{34}$$

The same procedure also applies to the case of constant heat flux. From Eqs. (28) and (30), we have

$$\frac{\mathrm{d}\hat{\delta}}{\mathrm{d}\hat{t}} = 1-\hat{\delta}^3 \tag{35}$$

The solution of this equation subject to $\hat{\delta}(0)=0$ is cast in an implicit form,

$$\hat{t} = \frac{1}{3}\ln\frac{\left(1+\hat{\delta}+\hat{\delta}^2\right)^{1/2}}{1-\hat{\delta}} + \frac{1}{\sqrt{3}}\tan^{-1}\frac{\sqrt{3}\hat{\delta}}{2+\hat{\delta}} \tag{36}$$

Again from Eqs. (28) and (30), $\hat{V}(\hat{t})$ is expressed as

$$\hat{V}(\hat{t}) = \frac{\tilde{\rho}-1}{\tilde{\rho}} + \frac{\hat{\delta}^3}{\tilde{\rho}} \tag{37}$$

The variation pattern of $\hat{\delta}(\hat{t})$ may not be perceived directly from Eq. (36). However, it can be calculated without difficulty because $\hat{\delta}$ is monotonic in $\hat{t}$.

A few observations can be made on the above solutions. The normalized liquid film thicknesses for both cases, i.e. Eqs. (32) and (36), are free completely from the characteristic parameters. Such independency plays an important role, as is shown later, in defining the unsteady period (time elapsed from the beginning to the steady state of melting) uniquely. In this sense, the present normalization seems to be successful. On the other hand, the solid descending velocity retains the density ratio. This is not caused by improper normalization, but is a natural consequence from the present model accounting for the solid–liquid density difference. Finally, an individual effect of all the parameters but the density ratio appears only in the steady solution. Only if the density ratio is fixed, the normalized solution represents a universal behavior of the unsteady close-contact melting.

The tangential force, Eq. (21), can be converted into the dimensionless form by defining a friction coefficient as [2,9]

$$f = \frac{F_x}{Mg} = \left(\frac{\tilde{\rho}\,Pr}{\tilde{g}\tilde{H}}\right)\tilde{U}\tilde{\delta}^{-1} \tag{38}$$

Once $\hat{\delta}(\hat{t})$ is known from the normalized solution, the variation of friction coefficient under specific conditions is readily calculated.

4. Discussion

4.1. Validation

One of the most desirable ways to validate an analytical model is to compare its result with precisely measured data, but no experiment on the unsteady close-contact melting has yet been reported. Fortunately, two sets of numerical data for each of the two heating modes are available. Listed in Table 1 are the

Table 1
Reference conditions used for validation and discussion

Heating mode	Constant wall temperature [4]	Constant heat flux [5]
Cross-sectional shape	Two-dimensional rectangular	Axisymmetric
Pr	13.44	13.44
$\tilde{H}$	1.0	1.0
$\tilde{g}$	5.521×10^{11}	5.521×10^{11}
G	4.0	1.5
$\tilde{\rho}$	1.0	1.09
Ste	1.266×10^{-2}	–
$\tilde{q}_w$	–	24.57

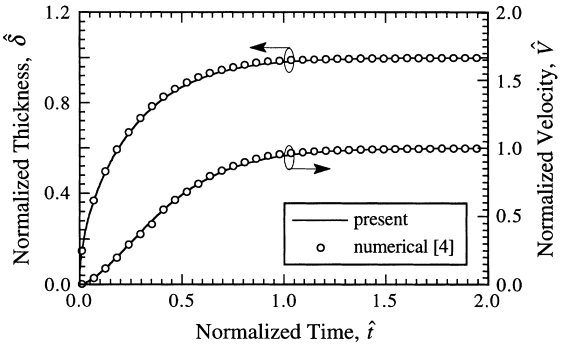

Fig. 2. Comparison of the present solution with the numerical data for constant wall temperature.

geometric configuration and dimensionless melting conditions considered in each of the numerical simulations [4,5]. Due to different geometry and characteristic length in each case, the function G appeared in the present solution should be replaced by a specific value. The previous study [1] has shown that it is 4 for the two-dimensional rectangular solid with infinite depth and 1.5 for the circular cross-section, respectively. The first one can be verified by examining the term $(L/R)^2G'$ in Eq. (22) under $R = L/2$ and $A = \infty$ along with the property of G' described earlier, whereas the second requires a separate axisymmetric analysis using $R = r$.

The evolutions of the liquid film thickness and solid descending velocity by the present solution are compared with those by the numerical data for constant wall temperature in Fig. 2 and for constant heat flux in Fig. 3, respectively, both in the normalized forms. Regardless of the heating mode, the present solution agrees excellently with the numerical data, which indicates that not only the simplifying assumptions introduced in modeling, but also the solution procedure are proper and valid. In particular, the present solution successfully resolves the effect of density difference in that $\hat{V}(0)$ is non-zero when $\tilde{\rho} \neq 1$, as shown in Fig. 3, which will be discussed further in the subsequent section. Another observation reads that the steady state is attained earlier in constant wall temperature than in constant wall heat flux on the normalized time scale.

In association with conducting an experiment of the unsteady close-contact melting, the following aspect deserves to note. A high degree of care should be paid either for keeping the wall temperature constant or for directly measuring the transient film thickness and solid descending velocity. In contrast, the supply of constant heat flux and measurement of the transient wall temperature seem to be relatively easy. Under the constant heat flux condition, Eq. (20) leads to the relation between the normalized film thickness and dimensionless wall temperature, i.e.

$$\frac{T_w - T_m}{T_{wc} - T_m} = \hat{\delta}(\hat{t}) \tag{39}$$

where T_{wc} is the wall temperature at the steady state. If $\hat{\delta}(\hat{t})$ is known from this relation and the measured temperature variation, the solid descending velocity $\hat{V}(\hat{t})$ can be calculated from Eq. (30). Neither $\hat{\delta}(\hat{t})$ nor $\hat{V}(\hat{t})$ needs to be measured directly.

4.2. Properties of the solution

In order to understand the basic characteristics of the unsteady close-contact melting, representative properties of the present solution are addressed. Plotted in Fig. 4 are the evolutions of the normalized film thickness for the two cases under consideration. Both curves show a common trend that they increase from 0 and asymptotically approach the steady state as the normalized time elapses, but the variation pattern depends on the heating mode. Note that the initial growth rate of the film thickness, $d\hat{\delta}(0)/d\hat{t}$, for constant wall temperature is infinity (Eq. (31)), whereas that for constant heat flux is unity

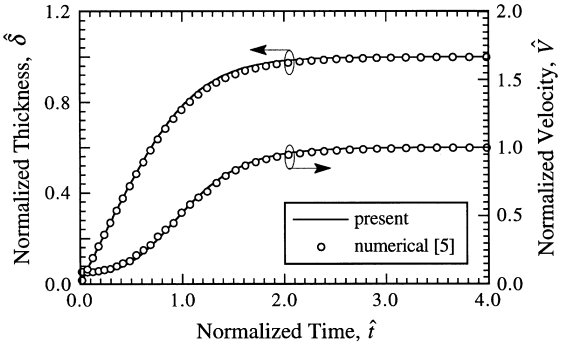

Fig. 3. Comparison of the present solution with the numerical data for constant wall heat flux.

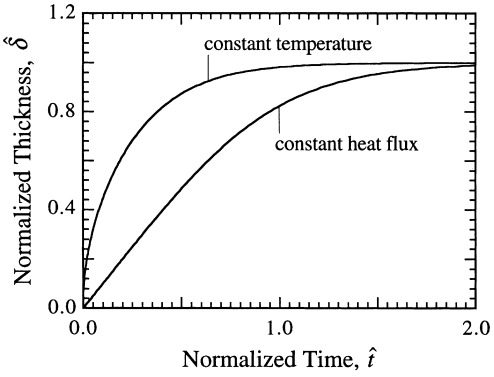

Fig. 4. Evolution of the normalized liquid film thickness for each heating mode.

(Eq. (35)). This also causes the afore-mentioned difference in the unsteady period between the two cases. In view of Eq. (39), the curve for constant heat flux also represents the wall temperature variation.

As evident in Eqs. (33) and (37), the transient behavior of the normalized solid descending velocity is affected essentially by the density ratio $\tilde{\rho}$. Fig. 5 illustrates its evolutions corresponding to three typical values of $\tilde{\rho}$ for each case. The dependence of $\hat{V}(\hat{t})$ on $\tilde{\rho}$ is more drastic in the case of constant wall temperature due to the infinite initial values when $\tilde{\rho} \neq 1$, especially during the early stage. The curves for $\tilde{\rho} < 1$ and $\tilde{\rho} = 1$ increase monotonically with time starting from $-\infty$ and 0, respectively, whereas that for $\tilde{\rho} > 1$ shows decreasing–increasing pattern from $+\infty$. In the case of constant heat flux, on the other hand, three curves vary similarly in pattern except that their initial values are different. Note that the initial values are finite in this case, i.e. $\hat{V}(0) = (\tilde{\rho} - 1)/\tilde{\rho}$. Here the important point is that every curve for $\tilde{\rho} \neq 1$ is discontinuous at $\hat{t} = 0$ in both cases. Such distinctive features of the solid descending velocity during the transient process have ever been reported in the numerical simulations. Hong [13] qualitatively predicted the decreasing–increasing pattern in close-contact melting of ice on an isothermal plate where $\tilde{\rho} = 1.09$, but a seeming numerical roughness makes it difficult to compare the simulated result with the present one quantitatively. The non-zero but finite value of $\hat{V}(0)$ in constant heat flux heating has already appeared in Fig. 3.

In view of the fact that there is no phase change at $\hat{t} = 0^-$, the predicted discontinuous phenomenon across $\hat{t} = 0$ is unlikely to occur in reality, possibly due to incomplete thermal contact, initial subcooling in the solid, viscous effect, and so on. Those factors, however, have been excluded in theoretical models, not only because they may not affect the fundamental nature of close-contact melting except at the beginning stage, but also because they are hard to model properly. Deducing from physical intuition, they seems to act on the actual process in a manner to smooth out the initial discontinuity. Another factor leading to the discontinuous behavior would be the neglection of inertia terms both in the force balance and in the momentum equations. However, considering that the afore-mentioned numerical simulations for $\tilde{\rho} \neq 1$ [5,13], where the full-scale equations were used, agree favorably with the analytical solutions even near $\hat{t} = 0$, the inertia seems to play a minor role throughout the whole process. To summarize, the present $\hat{V}(\hat{t})$ without accounting for those effects can be regarded as an asymptotic limit of the actual phenomenon from $\hat{t} = 0^+$ to $\hat{t} = \infty$. This deduction should be verified by a precise experiment.

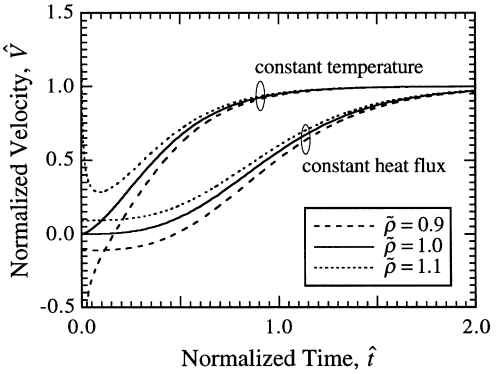

Fig. 5. Evolutions of the normalized solid descending velocity corresponding to three typical values of the density ratio for each heating mode.

Nevertheless, it is possible to explain the initial behavior of $\hat{V}(\hat{t})$ for $\tilde{\rho} \neq 1$ physically. Since the discontinuity disappears in case of $\tilde{\rho} = 1$, it can be attributed to the density ratio. Let us consider a situation that the specific volume of the liquid is larger than that of the solid, i.e. $\tilde{\rho} < 1$. As the heating begins, a part of the liquid generated by melting fills up the gap originally occupied by the solid, and the rest of the liquid, i.e. the excess liquid expressed by the term $(1 - \tilde{\rho})/\tilde{\rho}$ in Eq. (28), induces an abrupt rise of the pressure in the film because the gap is so thin that the longitudinal flow can not be still established. The pressure rise, in turn, bring forth a discontinuous ascending motion of the solid block. In the opposite situation ($\tilde{\rho} > 1$), the deficiency of the liquid causes a discontinuous descending motion at the very beginning of melting. Those phenomena attenuate sharply with growing the gap and intensifying the fluid flow through the gap while keeping the force balance.

One of the interesting results in the present analysis is the transient period. Since the transient state always entails the actual process, its effect needs to be estimated. As an example, consider an experiment to measure the steady close-melting rate under prescribed conditions. If we know a priori the time duration from the onset to the quasi-steady, the data acquired during the transient process can be discarded effectively. Due to the asymptotically approaching nature toward the steady state, the unsteady period, t_u, may be defined in various ways. In this context, a convenient aspect of the normalized film thickness, i.e. the independence on any parameters, is useful for defining $\hat{t}_u$, uniquely. For example, adopting the time corresponding to $1 - \hat{\delta} = 10^{-3}$ as $\hat{t}_u$, we have $\hat{t}_u \cong 1.727$ for constant wall temperature from Eq. (32) rewritten as

$$\hat{t} = \frac{1}{4}\ln\frac{1+\hat{\delta}^2}{1-\hat{\delta}^2} \tag{40}$$

and $\hat{t}_u \cong 2.788$ for constant heat flux from Eq. (36), re-

spectively. The unsteady period in real time, t_u, corresponding to $\hat{t}_u$ can be readily calculated. Specifically, t_u for each set of conditions in Table 1 is evaluated as about 11.4 and 8.5 s, respectively.

4.3. Aspect ratio of contact surface

Among the dimensionless parameters characterizing the present system, the aspect ratio of contact surface, A, needs further discussion, because it solely represents the three-dimensionality. The function G which is a function of A only can effectively take the place of the aspect ratio under the constraint of constant contact area. Fig. 6 shows the curve of $G(A)$. Since the coordinates x and y are commutative, as evident geometrically, G is symmetric about $A = 1$ (square cross-section). The function G attains its maximum at $A = 1(G(1) \cong 0.421731)$, and behaves like A^{-1} with approaching both of the extremes, i.e. for $A \ll 1$ and $A \gg 1$, in accordance to the property of G' described earlier. Owing to the symmetry, our discussion is made for $A > 1$. The circular cross-section is also considered here as a reference for constant contact area. It is easy to verify that this case corresponds to $G = 1.5/\pi$ by taking the characteristic length as $\pi^{1/2}r$ instead of r that has been used for an axisymmetric solid block [1]. The marked point in Fig. 6 means a circular equivalence of the rectangular cross-section having the same contact area.

Physically, the function G can be viewed, in an average sense, to represent the resistance of flow through the liquid film. When the contact area is kept constant, the mean flow path becomes shorter with increasing the aspect ratio, thereby making easy the outflow of liquid generated along the melting front. In order to investigate the effect of aspect ratio on the unsteady close-contact melting process, the evolutions of dependent variables corresponding to $A = 1$, 10 and circular cross-section are compared in Fig. 7 for constant wall temperature and in Fig. 8 for constant heat flux, respectively, under the same melting conditions listed in Table 1. All the results are expressed in terms of the dimensionless quantities to show the effect specifically. In both cases, the shorter the perimeter of contact surface, not only the thicker the steady film thickness, but also the longer the unsteady period. The solid descending velocity shows the same time dependency as the film thickness. Its steady values for the case of constant wall temperature increase with increasing the aspect ratio, whereas those for the case of constant heat flux are independent of the cross-sectional geometry, as is clear in Eq. (27). Note here that the relation between $\tilde{t}_u$ and A can be drawn easily based on the afore-mentioned uniqueness of $\hat{t}_u$. Regardless of the heating mode, it can be said that as the function G decreases, heat transfer is at least enhanced at the expense of the increase in flow friction (see Eq. (38)).

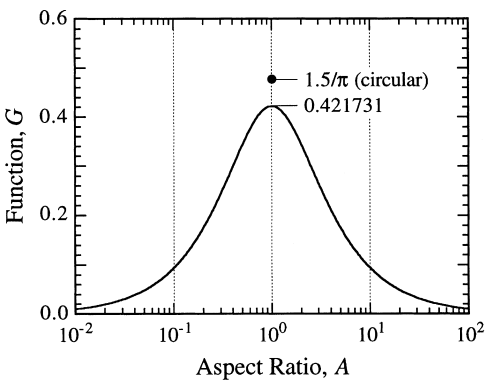

Fig. 6. Variation of the geometric function with respect to the aspect ratio of contact surface.

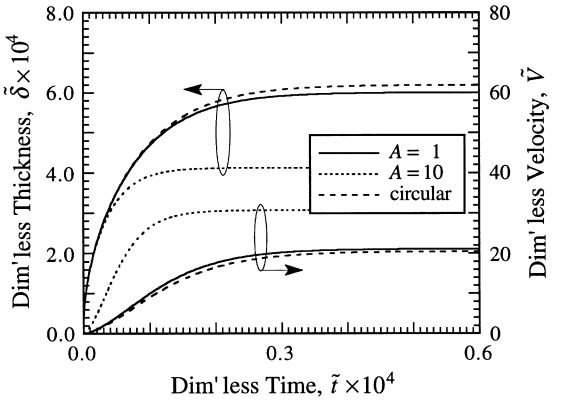

Fig. 7. Effect of the aspect ratio of contact surface on the evolutions of dependent variables in comparison to the case of circular cross-section for constant wall temperature.

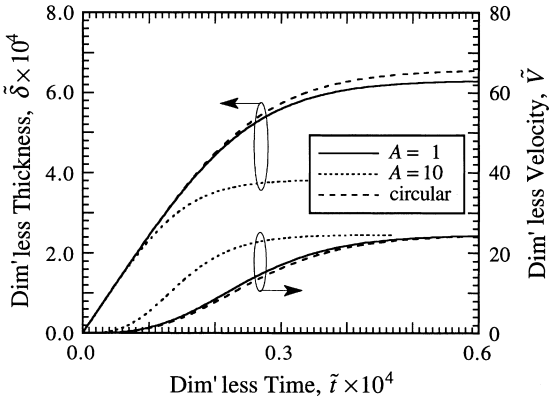

Fig. 8. Effect of the aspect ratio of contact surface on the evolutions of dependent variables in comparison to the case of circular cross-section for constant wall heat flux.

Table 2
The effect of geometric configuration on close-contact melting of a rectangular parallelepiped in reference to the cube with equal volume

Heating mode	Constant wall temperature	Constant heat flux
Total steady melting rate	$[G(A)/G(1)]^{-1/4}\tilde{H}^{-1/2}$	$\tilde{H}^{-1}$
Friction coefficient	$[G(A)/G(1)]^{-1/4}\tilde{H}^{-1/2}$	$[G(A)/G(1)]^{-1/3}\tilde{H}^{-1/3}$
Unsteady period	$[G(A)/G(1)]^{1/2}\tilde{H}^{-1}$	$[G(A)/G(1)]^{1/3}\tilde{H}^{-2/3}$

Since the effect of other parameters can be estimated easily via the steady solution implied in the normalized variables, as noted before, it is not dealt with here.

4.4. Application

The analysis performed so far has been based on a characteristic length appropriate for the case of constant contact area, and thereby the discussion has focused on a geometric function G defined in terms of the aspect ratio. However, such a length scale is not the only choice, but can be replaced by convenient alternatives within the framework of the present analysis.

As a representative example, consider the problem in which a constant-volume rectangular parallelepiped solid of variable contact area and height undergoes close-contact melting with relative motion. It is more convenient in this case to adopt $R = (LWH)^{1/3}$ instead of $R = (LW)^{1/2}$ as the characteristic length, because the former is constant. Substituting this into Eq. (22), we have a new dimensionless force balance equation,

$$\tilde{V} + (1-\tilde{\rho})\frac{\mathrm{d}\tilde{\delta}}{\mathrm{d}\tilde{t}} = \left(\frac{\tilde{g}\tilde{H}^2}{G\,Pr}\right)\tilde{\delta}^3 \tag{41}$$

while the others, i.e. Eqs. (24), (25) and (38), being kept unchanged. Since the only change by adopting the new length scale is $\tilde{H}^2$ in Eq. (41) in place of $\tilde{H}$ in Eq. (23), the steady solutions essentially remain the same as Eqs. (26) and (27) except the very change, thereby the normalized solutions being unaffected.

Table 2 presents the effects of geometric configuration on the selected characteristics of close-contact melting in reference to the cube ($\tilde{H} = 1; A = 1$) having the same volume, where the total steady melting rate is defined as $V_c LW$. As the contact area increases, i.e. with decreasing the height, melting is enhanced, the degree of which depends on the heating mode. That is, the total steady melting rate for constant wall temperature is proportional to the square root of the contact area, whereas that for constant heat flux is linear (note the relation between the contact area and dimensionless height, $LW = \tilde{H}^{-1}R^2$). These results stem from the fact that the temperature gradient at the melting front corresponding to variable contact area is dependent on the film thickness for constant wall temperature, but independent of it for constant heat flux. The same reason is attributable to the cases of the friction coefficient as well as the unsteady period. Regarding the effect of aspect ratio appeared in Table 2, the discussion made in conjunction with Figs. 7 and 8 seems to be sufficient. In fact, in close-contact melting of a constant-volume rectangular parallelepiped solid with relative motion, it can be understood qualitatively even without analysis that heat transfer and lubrication conflict with each other in response to the variation of contact area. However, in order to predict the quantitative effects or characteristics, the present analysis may be invoked.

5. Conclusions

An analytical approach has been carried out to predict the transient process of gravity-induced close-contact melting occurring between a rectangular parallelepiped solid initially at its melting temperature and a flat plate on which either constant temperature or constant heat flux is imposed. The present model accounts for not only relative motion between the solid block and the plate, but also the solid–liquid density difference of the phase change material. By introducing a number of already approved simplifications such as thin film approximation, we have derived a set of simultaneous first-order ordinary differential equations as the model equations.

Appropriate nondimensionalization and normalization in reference to the established steady solution yields simplified model equations that explicitly depend on the liquid-to-solid density ratio only. For each of the heating modes, we successfully obtained a compact-form analytical solution which agrees excellently with the available numerical data. Of particular interest is that the normalized liquid film thickness is independent of all the characteristic parameters, which serves as a theoretical basis to define the unsteady period uniquely. The solution is also capable of resolving the distinctive behavior of solid descending velocity for non-unity density ratios during the early stage of melting. This feature, which is consistent qualitatively with the existing numerical simulations, shows the importance of incorporating the density difference in the analysis.

The aspect ratio of contact surface affects the melting behavior in the form of a geometric function. This function is symmetric with respect to the square cross-section, and by itself characterizes the three-dimensionality of the present problem. As the perimeter of contact surface increases under the same contact area, heat transfer is shown to be at least enhanced along with the consistent increase in friction regardless of the heating mode. In this sense, a circular contact surface must be one of the limiting cases in close-contact melting for any heating mode. It was also revealed through a typical example that the characteristic length of the system is open to the user's choice within the extent of the change in the steady solution only. The present solution is applicable to predicting the case of simultaneous variation in height and cross-section of the solid.

Acknowledgements

This work was supported by grant No. 981-1106-042-1 through the Basic Research Program of the Korea Science and Engineering Foundation.

Appendix. Solution procedure for Poisson equation with homogeneous boundary conditions

Presented briefly is the solution procedure for the following Poisson equation appeared in association with the pressure distribution in the liquid film:

$$\frac{\partial^2 P}{\partial x^2} + \frac{\partial^2 P}{\partial y^2} = S \tag{A1}$$

$$P(\pm L/2, y) = 0; \qquad P(x, \pm W/2) = 0 \tag{A2}$$

where S is independent of both x and y. Based on the principle of superposition, the dependent variable can be decomposed as

$$P(x, y) = P_1(x) + P_2(x, y) \tag{A3}$$

$$\frac{\mathrm{d}^2 P_1}{\mathrm{d}x^2} = S, \qquad P_1(\pm L/2 = 0) \tag{A4}$$

$$\frac{\partial^2 P_2}{\partial x^2} + \frac{\partial^2 P_2}{\partial y^2} = 0, \quad P_2(\pm L/2, y) = 0; \quad P_2(x, \pm W/2) = -P_1(x) \tag{A5}$$

In this procedure, the independent variables are commutative with each other. A simple integration yields the solution of Eq. (A4). Due to the inherent symmetry, Eq. (A5) constitutes an eigenvalue problem, the solution of which can readily be derived using the method of separation of variables. The final solution emerges as

$$P(x, y) = S\left[\frac{1}{2}\left\{x^2 - \left(\frac{L}{2}\right)^2\right\} + \sum_{n=0}^{\infty} K_n \cos(\beta_n x)\cosh(\beta_n y)\right] \tag{A6}$$

where the eigenvalues and the Fourier coefficients, respectively, are

$$\beta_n = \frac{(2n+1)\pi}{L} \tag{A7}$$

$$K_n = \frac{(-1)^n 4}{L\beta_n^3 \cosh(\beta_n W/2)} \tag{A8}$$

References

[1] M.K. Moallemi, B.W. Webb, R. Viskanta, An experimental and analytical study of close-contact melting, J. Heat Transfer 108 (1986) 894–899.
[2] A. Bejan, The fundamentals of sliding contact melting and friction, J. Heat Transfer 111 (1989) 13–20.
[3] A. Bejan, Contact melting heat transfer and lubrication, Adv. Heat Transfer 24 (1994) 1–38.
[4] H. Hong, A. Saito, Numerical method for direct contact melting in transient process, Int. J. Heat Mass Transfer 36 (1993) 2093–2103.
[5] A. Saito, H. Kumano, S. Okawa, K. Yamashita, Analytical study on transient direct contact melting phenomena, Trans. JAR (in Japanese) 13 (1996) 97–108.
[6] M. Bareiss, H. Beer, An analytical solution of the heat transfer process during melting of an unfixed solid phase change material inside a horizontal tube, Int. J. Heat Mass Transfer 27 (1984) 739–746.
[7] S.K. Roy, S. Sengupta, The melting process within spherical enclosures, J. Heat Transfer 109 (1987) 460–462.
[8] A. Bejan, Single correlation for theoretical contact melting results in various geometries, Int. Comm. Heat Mass Transfer 19 (1992) 473–483.
[9] A. Bejan, in: Convection Heat Transfer, 2nd ed., Wiley, New York, 1995, pp. 434–455.
[10] G.K. Batchelor, in: An Introduction to Fluid Dynamics, Cambridge University Press, Cambridge, UK, 1967, pp. 219–222.
[11] K. Taghavi, Analysis of direct-contact melting under rotation, J. Heat Transfer 112 (1990) 137–143.
[12] H. Yoo, H. Hong, C-J. Kim, Effects of transverse convection and solid–liquid density difference on the steady close-contact melting, Int. J. Heat Fluid Flow 19 (1998) 368–373.
[13] H. Hong. Heat transfer in direct contact melting process. Ph.D. thesis, Tokyo Institute of Technology, Tokyo, Japan, 1993.